Apparent Debye−Huckel Electrostatic Effects in the Folding of a Simple, Single Domain Protein†

Miguel A. de los Rios‡ and Kevin W. Plaxco*,‡,§

Department of Chemistry and Biochemistry, and Interdepartmental Program in Biomolecular Science and Engineering, University of California, Santa Barbara, Santa Barbara, California 93106

Received July 21, 2004; Revised Manuscript Received November 11, 2004

ABSTRACT: We have monitored the effects of salts and denaturants on the folding of the simple, two-state protein FynSH3. As predicted by Debye−Huckel limiting law, both the stability and (log) folding rate of FynSH3 increase nearly perfectly linearly ($r^2 > 0.99$) with the square root of ionic strength upon increasing concentrations of the relatively nonchaotropic salt sodium chloride. The stability of FynSH3 is also linear in square root ionic strength when the relatively nonchaotropic salts sodium bromide, potassium bromide, and potassium chloride are employed. Comparison of the kinetic and equilibrium effects of sodium chloride suggests that the electrostatic interactions formed in the folding transition state are approximately 50% as destabilizing as those formed in the native state, presumably reflecting the more compact nature of the latter. In contrast, the relationship between concentration and folding kinetics is more complex when the highly chaotropic salt guanidine hydrochloride (GuHCl) is employed. At moderate to high GuHCl concentrations the net effect of the linear, presumably chaotrope-induced deceleration and the presumed, square root-dependent ionic strength-induced acceleration is well approximated as linear, thus accounting for the observation of "chevron behavior" (log folding rate linear in denaturant concentration) typically reported for the folding of single domain proteins. At very low GuHCl concentrations, however, significant kinetic rollover is observed. This rollover is reasonably well fitted as a sum of a linear, presumably chaotropic effect and a square root-dependent, presumably electrostatic effect. These results thus not only provide insight into the nature of the folding transition state but also suggest that caution is in order when extrapolating GuHCl-based chevrons to estimate folding rates in the absence of denaturant and in interpreting deviations from chevron linearity as evidence for non-two-state kinetics.

Because proteins are polyampholytes (mixed charged polymers), both their thermodynamic stability and folding kinetics depend strongly on solvent ionic strength. Historically, however, it has proven difficult to define precisely the extent to which ionic strength affects folding. The difficulty arises because, in addition to the electrostatic consequences of increased ionic strength, other properties of salts also contribute to the thermodynamics of the native and folding transition states. For example, the binding of ions to specific, saturable sites on the folded or unfolded state will stabilize or destabilize the native state, respectively, leading to a hyperbolic relationship between folding free energy and salt concentration (e.g., ref *1*). Similarly, because the hydrophobic effect dominates folding, the chaotropic or kosmotropic behavior of added salts [as, for example, qualitatively defined by the Hofmeister series (*2*)] strongly affects both protein stability and folding rates. For "purely" chaotropic or kosmotropic effectors (such as urea or glycerol), a strongly linear relationship between native state stability (or log folding rate) and concentration is generally observed for smaller proteins (e.g., refs *3* and *4*). For non-two-state folding, however, more complex, nonlinear relationships are sometimes observed as, for example, increasing amounts of chaotrope destabilize aggregates or discrete folding intermediates (e.g., ref *5*). Complex, nonlinear relationships are also sometimes observed when a salt produces both ionic strength and, particularly at higher concentrations, chaotropic or kosmotropic effects (e.g., ref *6*). In the presence of these complicating effects, it is generally difficult to ascertain the extent to which salt-induced changes in folding are a consequence of the purely electrostatic effects of altering ionic strength.

The effect of ionic strength on electrostatic forces is given by the Debye−Huckel limiting law, which describes the cloud of counterions that forms around a point charge in solution and thus screens Coulombic interactions. The efficiency of this screening is related to the thickness of the counterion atmosphere, which in turn is dependent on the square root of the ionic strength (*7*). If the electrostatic interactions in a protein are net destabilizing, the Debye−Huckel screening will increase the stability of the native protein relative to the more expanded, unfolded state (even if some residual electrostatic interactions remain in the unfolded state), with the change in stability varying with the

† This work was supported by NIH Grant R01GM62868-01A1.

* To whom correspondence should be addressed: (805) 893-5558 (phone); (805) 893-4120 (fax); kwp@chem.ucsb.edu (e-mail).

‡ Department of Chemistry and Biochemistry, University of California, Santa Barbara.

§ Interdepartmental Program in Biomolecular Science and Engineering, University of California, Santa Barbara.

10.1021/bi048444l CCC: $30.25
Published on Web 01/07/2005

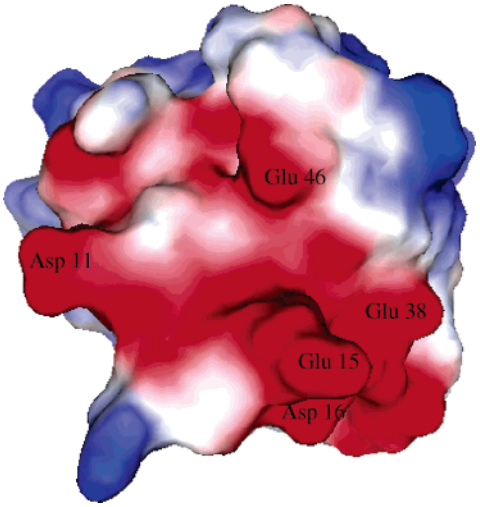

FIGURE 1: The electrostatic structure of native FynSH3 is indicated, with 11 negatively and 5 positively charged residues at the pH employed here. A cluster of sequence-distant, negatively charged residues is apparent that presumably contributes to the net unfavorable role that electrostatics play in the folding of this protein. Similar electrostatic destabilization in the cold shock family of proteins is well established (*6*).

square root of the ionic strength. Similarly, in the absence of confounding binding, chaotropic or kosmotropic effects, the electrostatic screening of salt should produce a linear relationship between log folding rates (proportional to the relative free energy of the folding transition state) and the square root of the ionic strength over the concentration range in which the Debye−Huckel limiting law is valid.

In an effort to enhance our understanding of the role that electrostatics play in folding, we have characterized the refolding of the FynSH3 domain in the presence of a range of ionic and chaotroic cosolvents. These include the neutral, relatively nonchaotropic or kosmotropic salts NaCl, NaBr, KCl, and KBr, the uncharged chaotrope urea, and the highly chaotropic salt guanidine hydrochloride (GuHCl).[1] The FynSH3 domain (Figure 1) is a simple, single-domain protein that exhibits two-state kinetic and equilibrium folding (*8*). Because of its simplicity, FynSH3 appears to be an ideal system with which to deconvolute the potentially confounding contributions of salts to folding and to therefore ascertain the role that electrostatic interactions play in protein stability and folding kinetics.

MATERIALS AND METHODS

Full-length (54 residues) FynSH3 was employed for experiments studying the effects of GuHCl, NaBr, KBr, and KCl, and the truncation mutation NΔ3-FynSH3 was employed for use with urea and NaCl. These choices were motivated by the observation that, whereas the full-length protein does not unfold completely even in saturated urea, the three-residue, amino-terminal truncation mutant NΔ3-FynSH3 is sufficiently destabilized that it unfolds in urea at salt concentrations as high as 2 M NaCl. While we monitored not the effects of several monovalent salts on folding, we did investigate any polyvalent salts, as polyvalent cations very frequently exhibit specific binding (to ligands such as glutamate and aspartate), and polyvalent anions (such as sulfate) invariably fall far from the center of the Hofmeister series and thus exhibit strong chaotropic or kosmotropic effects.

Both the full-length and truncated FynSH3 domains retain two-state folding characteristics as determined by equilibrium denaturation monitored by circular dichroism at 220 nm and by kinetic analysis of folding and unfolding as monitored by stopped-flow fluorometry (see below). Both proteins were expressed from pET15b vector in *Escherichia coli* BL-21-(DE3) pLysS cells. Purification consisted of a standard Ni protocol (Qiagen) followed by exhaustive dialysis against 10 mM NH_4HCO_3 and lyophilization. The amino-terminal six-His tag was retained in both constructs; the pH employed is sufficiently high that the tag is uncharged. All experiments were performed in 10 mM Tris, pH 8.1. As 8.1 is the pK_a of Tris in the limit of 0 M ionic strength (at 25 °C), the buffer contributes ~0.005 M to the ionic strength in the absence of added salt. While this contribution will decrease slightly at higher ionic strengths (the pK_a of Tris increases slightly with increasing ionic strength), this change is relatively minor and has been ignored.

Folding Free Energy as a Function of NaCl. Because NΔ3-FynSH3 is relatively unstable, it does not exhibit a sufficient folded baseline in the absence of salt (Figure 2, right). Similarly, in the presence of 2 M NaCl the protein is so stable that even saturating urea concentrations do not produce a significant unfolded baseline. We thus employed the following approach and assumptions in fitting urea denaturation curves to determine folding free energy at various salt concentrations. Fitting all of the curves to the relevant equilibrium unfolding equations [with sloped baselines (*9*)], we find that the slopes and intercepts of both baselines are within error of one another and do not exhibit any systematic variations as a function of salt concentration (data not shown). The urea *m*-values obtained from these fits are also closely similar and also fail to exhibit any systematic variation with salt concentration (data not shown), an effect that has been reported previously (e.g., refs *10* and *11*). That said, the folded baselines of the four lowest NaCl concentrations, the unfolded baselines of the four highest NaCl concentrations, and the *m*-values of the two lowest and two highest NaCl concentrations are extremely poorly constrained. We thus assumed that the average unfolded baseline of the five lowest NaCl samples, the average folded baseline of the five highest NaCl samples, and the mean *m*-value of the five intermediate NaCl concentrations held for the entire data set. Each curve was thus fit to the equation:

$$\theta = (-0.437[\text{urea}] - 8.63)/(1 + \exp(\Delta G_u + 0.6075[\text{urea}]/RT)) + 0.743[\text{urea}] - 15.83 \quad (1)$$

where the first two terms are the slope and intercept, respectively, for the difference between the mean folded and unfolded baselines, the last two terms are the mean slope and intercept of the unfolded baseline, and the value 0.6075 [in kcal/(mol·M)] is the mean equilibrium urea *m*-value for the mutant. The fits to this *single-parameter* equation are excellent (all $r^2 > 0.93$, median $r^2 = 0.99$), suggesting that our assumption of fixed baselines and *m*-values is valid and producing ΔG_u constrained to within ±0.04 kcal/mol.

[1] Abbreviation: GuHCl, guanidine hydrochloride.

Folding Free Energy as a Function of NaBr, KBr, and KCl. Fluorescence-detected (excitation 280 nm, emission above 320 nm) urea titrations were employed to measure the effects of NaBr, KBr, and KCl on the stability of the full-length FynSH3 construct (Figure 3). The data were fitted to a standard two-state equilibrium unfolding equation with a fixed intercept for the folded baseline (the spectrometer output was arbitrarily set to unity at the start of each titration) and with the urea *m*-value for this construct fixed at the mean value of 0.57 kcal/(mol·M). With the exception of the zero added salt titration, the unfolded baselines were extremely short, and the unfolded baseline slopes were thus fixed at zero. This is clearly an approximation, however, and limits the precision with which free energy is determined under such conditions.

Folding Kinetics as a Function of NaCl. Observed relaxation rates (Figure 4) were determined at a final urea concentration of 0.82 M and NaCl concentrations ranging from 0.05 to 2 M. Folding was initiated by a rapid dilution of 9 M urea plus NaCl into a solution of equal concentrations of NaCl but lacking urea. Rates were monitored by tryptophan fluorescence changes using an APP SX.18MV stopped-flow fluorometer (Applied Photophysics, Leatherhead, England). Due to the relative instability of NΔ3-FynSH3 at low NaCl concentrations (Figure 2) the assumption that $k_{obs} \approx k_f$ does not hold. For this reason we calculated k_f (Figure 4, right) from k_{obs} and the known ΔG_u (see above) using the equation:

$$k_f = k_{obs}/[1 + \exp(\Delta G_u/RT)] \quad (2)$$

The urea- and GuHCl-derived chevrons were generated by standard methods using an APP stopped-flow fluorometer (Figures 5 and 6). Folding rates in the folding arm of the GuHCl chevron were determined by two methods. Most of the data were determined by refolding protein that had been denatured in 4.5 M GuHCl via rapid dilution into solutions of varying GuHCl concentration. The rollover portion of the arm was determined by monitoring refolding of urea-denatured protein in the presence of a given amount of GuHCl and varying amounts of urea. The folding rate in the presence of that amount of GuHCl was then derived by extrapolating the data to 0 M urea. To test the validity of this approach, refolding rates were determined using both methods for a number of GuHCl concentrations. No significant deviations are observed (Figure 6; overlapping squares and diamonds). The unfolded arm of the chevron was determined by unfolding protein in increasing concentrations of GuHCl. Reported parameters and confidence intervals were obtained via nonlinear least-squares fitting (Kaleidagraph, Abelbeck Software, Inc.). Kinetic data were fitted as the logarithm of rates (see eqs 2−4) in order not to overweight the fastest (and thus most poorly measured) rates. Because many of the relevant variables are highly cross-correlated (e.g., the various *m*-values), these confidence intervals are at best a very crude measure of standard error. For this reason we have not estimated confidence intervals for the various Tanford β-values; as the ratio of two cross-correlated parameters, it is very difficult to accurately assign realistic confidence intervals to these values.

RESULTS

We have employed three classes of cosolvents and two proteins in our studies. The first set of cosolvents, NaCl, KCl, NaBr, and KBr, are relatively nonchaotropic and nonkosmotropic salts; all four ions fall near the middle of their respective Hofmeister series. The next cosolvent, urea, is a nonionic but highly chaotropic agent. As such, it significantly destabilizes compact protein conformations, with an efficiency that closely parallels the hydrophobic surface area exposed upon unfolding (*12*). The behavior of the last cosolvent, GuHCl, is more complex. Like salts of sodium, potassium, chloride, and bromide, GuHCl is highly dissociated in aqueous solution. Unlike these other four ions, however, guanidinium is near the chaotropic extreme of the Hofmeister cation series. The proteins we have employed are the full-length FynSH3 domain and a destabilized truncation mutant. The mutant, NΔ3-FynSH3, was employed for some experiments because the full-length protein does not completely unfold in urea at ionic strengths above ~250 mM. NMR, fluorescence, and circular dichroism measurements indicate that the native fold of the mutant is indistinguishable from that of the full-length protein (B. Gillespie, J. Kohn, and K. W. Plaxco, unpublished results).

NaCl increases the stability of the NΔ3-FynSH3 domain (Figure 2), suggesting that, in net, electrostatic interactions in the native state are repulsive and thus favor the expanded, unfolded state. Consistent with the predictions of the Debye−Huckel limiting law, the folding free energy of NΔ3-FynSH3 is nearly perfectly linear ($r^2 = 0.998$) in square root of ionic strength (Figure 2, right), fitting the equation:

$$\Delta G_u(I) = \Delta G_u^\circ + m_{eq}' I^{1/2} \quad (3)$$

(where I is the ionic strength in M and ΔG_u° is the folding free energy in the limit of 0 M ionic strength) up to the highest salt concentrations we can investigate (urea does not unfold the protein above 2 M NaCl). The linearity of the free energy versus square root of ionic strength suggests that, in reference to Debye−Huckel theory and by analogy to the well-known *m*-value defined for denaturants, we can define an equivalent value, designated m_{eq}', for the effect of ionic strength on stability. The observed m_{eq}' value is 2.90 ± 0.07 kcal/(mol·M$^{1/2}$).

A hallmark of electrostatic screening is that the effect is independent of the identity of the ion employed to alter the ionic strength (with the potentially serious caveat that specific binding or Hofmeister effects might vary, leading to ion-specific deviations from simple Debye−Huckel behavior). To test this, we have monitored the effects of sodium bromide, potassium bromide, and potassium chloride on the stability of FynSH3, albeit not without significant technical hurdles. For example, bromide absorbs strongly in the far-UV, precluding the use of CD to monitor folding, and the baseline fluorescence of FynSH3 varies strongly with salt concentration. To minimize these effects, we explored the full-length protein (to obtain a fittable folded baseline at low salt) and limited our studies to salt concentrations below 0.25 M (to obtain fittable unfolded baselines). Despite these limitations the free energy values we obtained are relatively poorly constrained. Nevertheless, we find that the behavior of all three of these salts is effectively indistinguishable from

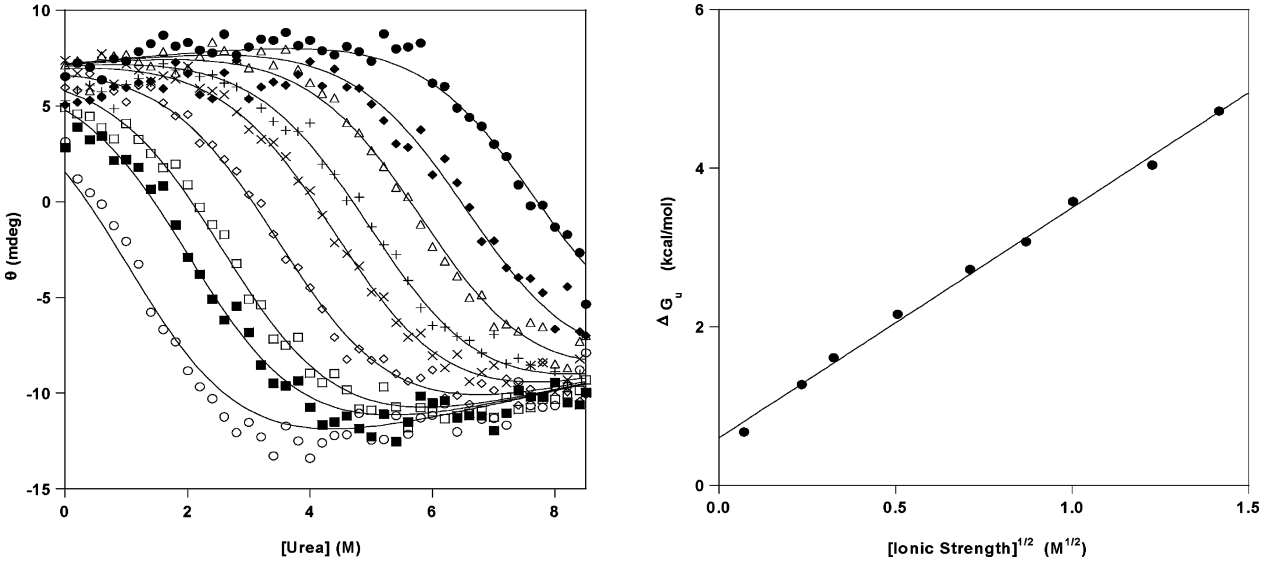

FIGURE 2: The stability of NΔ3-FynSH3 increases with increasing NaCl concentration. (Left) Equilibrium urea denaturation transitions were determined by monitoring circular dichroism at 220 nm. The fits (solid lines) assume common, fixed baselines and a fixed *m*-value. Folding free energy is thus the only unconstrained variable in the fits. NaCl concentrations are, from left to right, 0, 0.05, 0.1, 0.25, 0.5, 0.75, 1.0, 1.5, and 2.0 M. (Right) As predicted by the Debye−Huckel limiting law, the folding free energy of NΔ3-FynSH3 is linearly dependent on the square root of ionic strength ($r^2 = 0.998$). Fits of the concentration dependence of folding free energy to hyperbolic (as predicted for specific ion binding) or linear (as generally observed for chaotropic and kosmotropic effects) relationships are weaker ($r^2 < 0.987$ and $r^2 < 0.920$, respectively), despite the inclusion of an additional floating parameter in the former. Fits to the extended Debye−Huckel equation (*40*) are also not statistically significantly improved (data not shown).

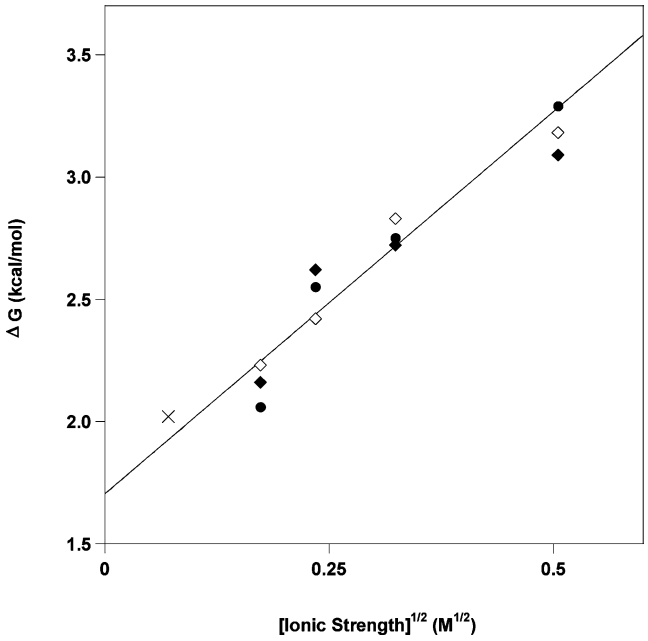

FIGURE 3: The folding free energy of full-length FynSH3 is also approximately linear in square root of ionic strength when NaBr (filled circles), KCl (open diamonds), or KBr (filled diamonds) is employed to modulate the ionic strength. The solid line represents a simultaneous fit of all of the data ($r^2 = 0.95$) and produces a slope (m_{eq}') within error of that observed for the shorter, NΔ3-FynSH3 construct when NaCl is employed as the salt. The free energy values obtained using these salts are relatively poorly constrained due to systematic errors introduced by extremely limited folding and unfolding baselines; sensitivity analysis indicates that typical errors are ~0.1 kcal/mol (data not shown). Denoted by a × is the free energy observed in the absence of added salt (at an ionic strength of 5 mM arising due to the buffer).

that of NaCl (Figure 3); all three stabilize FynSH3 with a square root dependence on ionic strength and with a mean m_{eq}' value of 3.13 ± 0.22 kcal/(mol·M), which is within error of the value observed for the truncated, NΔ3-FynSH3 construct in NaCl.

Sodium chloride accelerates the urea-jump relaxation kinetics of FynSH3 (Figure 4). The relaxation kinetics of the NΔ3-FynSH3 mutant increase ~5-fold as NaCl concentration is increased from 0 to 2 M (final urea concentration held constant at 0.82 M) apparently without reaching a plateau. The mutant is, however, relatively unstable at low ionic strength, and thus both the folding and unfolding processes contribute significantly to the observed relaxation kinetics. Knowledge of the protein's stability allows us to deconvolute these two contributions to the relaxation rate and thus to determine the folding rate of the protein as a function of salt concentration.

Using the folding free energy and the observed relaxation rates at each NaCl concentration, we can calculate folding rates as a function of ionic strength. We find that the logarithm of the NΔ3-FynSH3 folding rate is linear in square root of ionic strength ($r^2 = 0.993$):

$$\ln k_f(I) = \ln k_f^\circ + m_f' I^{1/2}/RT \quad (4)$$

where k_f° is the folding rate in the limit of 0 M ionic strength (Figure 4, right). The extent to which salt stabilizes the folding transition state (m_f', by analogy to the denaturant-defined m_f) is 1.40 ± 0.06 kcal/(mol·M$^{1/2}$). The ratio of this value to the NaCl-derived m_{eq}' (a ratio analogous to the so-called Tanford β-value and thus denoted β_{DH}) is 0.48. Assuming that this results purely from electrostatic screening effects, this ratio suggests that, while they are more repulsive than those in the unfolded state, the electrostatic interactions formed in the folding transition state are significantly less repulsive than those formed in the native state. This is consistent with the dimensions of the folding transition state being between those of the compact native state and the relatively expanded denatured state.

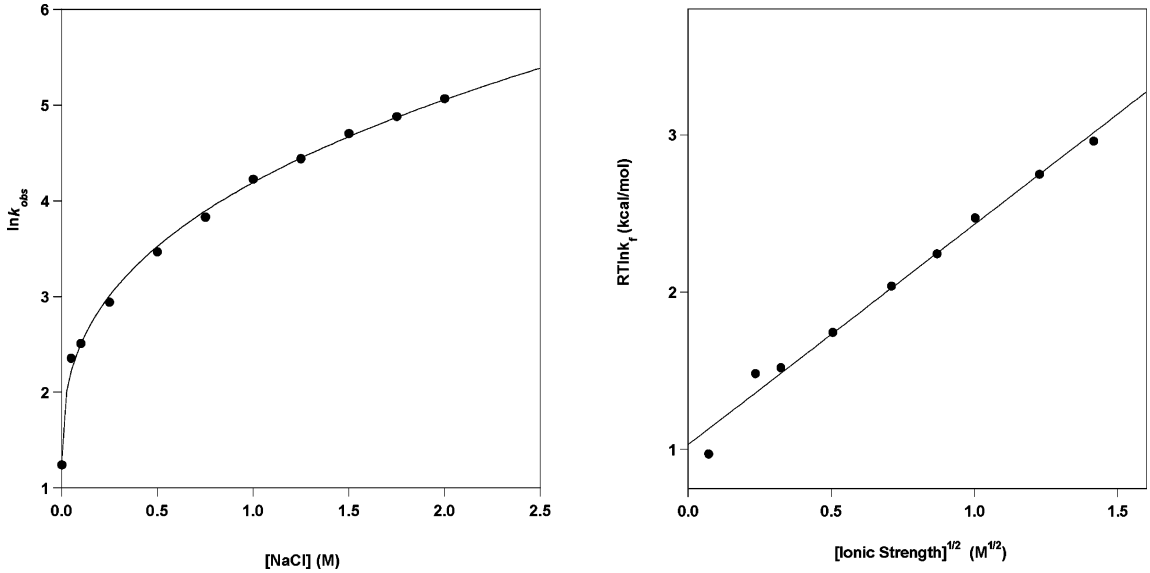

FIGURE 4: The folding kinetics of NΔ3-FynSH3 accelerate with increasing NaCl concentration. (Left) The solid line represents a fit of the natural logarithm of the observed relaxation rate (ln k_{obs}) to a power law relationship with an exponent of 0.37 ± 0.02 (r^2 = 0.994). In contrast, these observations are somewhat more poorly fit by the square root relationship predicted by the Debye−Huckel limiting law (r^2 = 0.977; data not shown) and much more poorly fit by the linear relationship typically observed for chaotropic agents (r^2 = 0.88; data not shown). At low ionic strength, however, NΔ3-FynSH3 is relatively unstable, and thus unfolding rates contribute to k_{obs}, confounding the relationship between rates and ionic strength. Correcting for this effect (right), we observe that the kinetic folding barrier of NΔ3-FynSH3 is, as predicted by the Debye−Huckel limiting law, linearly dependent on the square root of ionic strength (r^2 = 0.993). A constant final urea concentration of 0.82 M was employed in these experiments.

We have monitored the effects of the nonionic chaotrope urea on full-length FynSH3. The data are well fitted (r^2 = 0.995) to a two-state chevron equation:

$$\ln k_{obs} = \ln[\exp(\ln k_f^\circ + m_f[\text{urea}]/RT) + \exp(\ln k_u^\circ + m_u[\text{urea}]/RT)] \quad (5)$$

where k_f° and k_u° are the folding and unfolding rates in the absence of denaturant and m_f and m_u are the kinetic *m*-values for folding and unfolding, respectively (Figure 5). The Tanford β-value, $\beta_T = m_f/(m_f - m_u)$, is ∼84%, suggesting that approximately this fraction of the hydrophobic surface area buried in the native state is buried in the transition state. This suggests that, in the folding transition state of FynSH3, hydrophobic interactions may be more significantly consolidated than the equivalent electrostatic interactions.

The effects of the chaotropic salt GuHCl are, not surprisingly, more complex than those of either the effectively nonchaotropic/kosmotropic salt NaCl or the nonionic chaotrope urea. Using the full-length FynSH3 domain, we see a nearly perfect linear relationship between log k_f and GuHCl concentration above 0.5 M denaturant (Figure 6). At lower denaturant concentrations significant rollover is observed, such that at below 0.2 M GuHCl increases in denaturant concentration *accelerate* folding. Assuming that the entire GuHCl chevron, including the low-denaturant rollover region, can be described as the sum of an effect that is linear in GuHCl concentration (representing the chaotropic nature of the salts) and an effect that goes with the square root of ionic strength (representing the putative Debye−Huckel effects), the observed relaxation rates should relate to GuHCl concentration via the equation:

$$\ln k_{obs} = \ln[\exp(\ln k_f^\circ + m_f[\text{GuHCl}]/RT + m_f' I^{1/2}/RT) + \exp(\ln k_u^\circ + m_u[\text{GuHCl}]/RT + m_u' I^{1/2}/RT)] \quad (6)$$

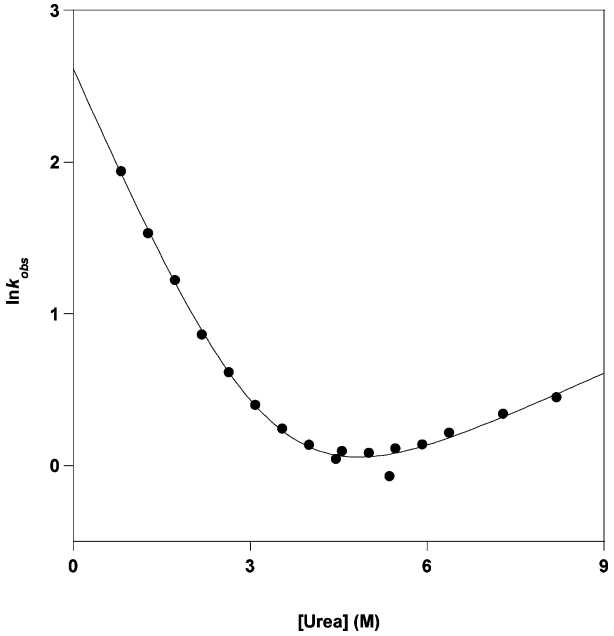

FIGURE 5: Linear chevron behavior is observed when full-length FynSH3 is folded or unfolded in the presence of the uncharged chaotrope urea. The Tanford β_T value derived from these data demonstrates that urea destabilizes the folding transition state only ∼84% as effectively as it destabilizes the native state.

where m_f and m_u are the kinetic folding and unfolding *m*-values associated with the chaotropic effect and m_f' and m_u' are the kinetic *m*-values associated with the ionic character of GuHCl (Table 1). If we assume that the m_f' and m_u' (as $m_{eq}' - m_f'$) of NaCl and GuHCl are identical (as should be the case for a purely ionic strength effect that depends on the charge, rather than the chemistry, of the ion), the linear chevron with rollover curve is well fitted by eq 6 (Figure 6; r^2 = 0.994). From this fit we estimate that the purely chaotropic effects of GuHCl produce a Tanford β_T

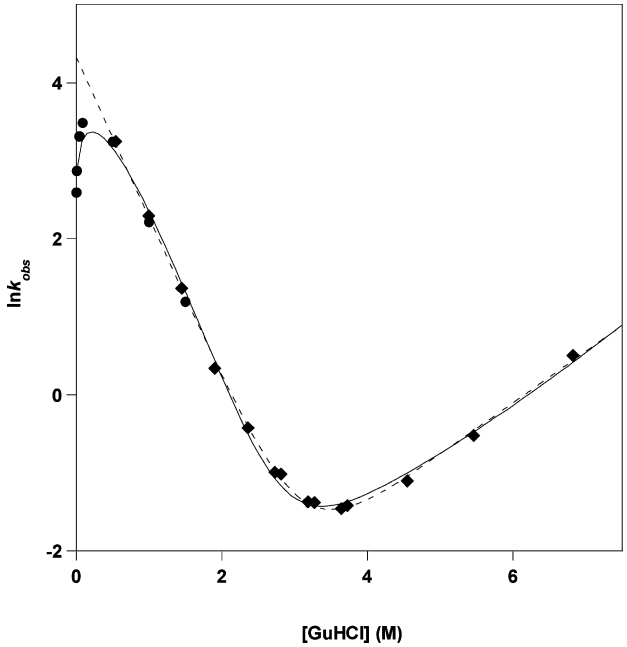

FIGURE 6: While linear chevron behavior is observed above 1 M GuHCl, significant kinetic rollover is observed in the folding of full-length FynSH3 at lower denaturant concentrations. This deviation arises because, in addition to being a chaotrope (which produces a linear relationship between ln k and denaturant concentration), GuHCl is also a salt, which produces square root Debye−Huckel dependence. The solid line is a fit to the sum of these two effects (eq 4), assuming that the ionic effects of NaCl and GuHCl are identical (i.e., using NaCl-derived m_f' and m_u' values obtained from the data in Figures 2 and 4). The reasonably good fit of this line suggests that Debye−Huckel electrostatic effects play a significant role in generating the observed rollover, although a hyperbolic, specific binding effect cannot be ruled out. A fit limited to the linear region of the chevron (dashed line) largely ignores the rollover effects and consequently overestimates the folding rate in the absence of denaturant by a factor of ~5. The diamonds denote directly measured rates, whereas the circles denote urea-extrapolated rates.

of 0.71, which coincides reasonably well with the 0.84 observed for the purely chaotropic agent urea. If we allow m_f' and m_u' to float, rather than assuming that the ion charge-mediated effects of NaCl and GuHCl are identical, we find that the fitted values obtained from eq 6 are poorly constrained (Table 1). This occurs because an effect that goes with the square root of ionic strength is reasonably well approximated as linear at the high GuHCl concentrations employed in the unfolding arm of the chevron and, thus, m_u and m_u' are highly cross-correlated. Nevertheless, the chaotropic β_T and putatively ionic β_{DH} values we derive from this fit, $\beta_T \approx 0.72$ and $\beta_{DH} \approx 0.50$, respectively, coincide reasonably well with the equivalent values obtained with urea ($\beta_T = 0.84$) and NaCl ($\beta_{DH} = 0.48$), providing additional support for the additivity of the ionic and chaotropic effects of GuHCl.

DISCUSSION

The nonchaotropic salts NaCl, NaBr, KCl, and KBr modulate the stability and folding kinetics of the FynSH3 domain with a linear dependence on the square root of ionic strength that is consistent with the Debye−Huckel limiting law. The observed square root dependence is inconsistent with either specific ion binding events (which would produce a hyperbolic relationship that is likely to vary from ion to ion) or chaotropic/kosmotropic effects (which produce linear relationships). That their free energies fall with increasing salt concentration suggests that, for both the native and folding transition states of this protein, electrostatic interactions are net destabilizing, perhaps because of a prominent cluster of sequence-distant negatively charged residues in the native state (Figure 1). The ratio of the magnitude of these effects suggests that the electrostatic contribution to the relative stability of the folding transition state, β_{DH}, is ~50% that of its contribution to the native state. This is consistent with the expanded nature of the transition state relative to the native state. The equivalent ratio of kinetic to equilibrium m-values derived using chaotropes, β_T, is ~70−80%, which suggests that the nativelike hydrophobic interactions in the transition state are significantly more "consolidated" than the equivalent electrostatic interactions.

While salt-induced increases in protein stability are relatively common (e.g., refs *10*, *11*, and *13*−*17*), the Debye−Huckel behavior reported here is perhaps surprising given that the relevant theory is generally thought to hold only under extremely dilute conditions. Debye−Huckel scaling of folding free energy may, nevertheless, be a fairly common phenomenon. For example, the stability of the S-peptide/S-protein complex (*14*), MetJ (*18*), and the H2A−H2B histone dimer (Figure 6 of ref *10*) have been shown to depend on the square root of ionic strength when NaCl is employed. Similarly, while the ability of Debye−Huckel behavior to account for the salt dependencies of their stability has not been reported, inspection of the relevant published data suggests that the equilibrium folding of RNase T1 (Figure 2 of ref *19*, but see also ref *20*), RNase A (Figure 2 of ref *20*), cspB (Figure 3 of ref *15*), the Caspase recruitment domain (Figure 4 of ref *15*), and apoflavodoxin (Figure 4, lower panel, of ref *21*) also exhibits at least approximately square root dependencies on ionic strength across widely ranging NaCl concentrations. Given the generally held opinion that the Debye−Huckel limiting law fails above even modest salt concentrations, the generality of this observation and, indeed, whether it truly reflects Debye−Huckel electrostatic effects may be of significant interest to the theoretical community.

The issue of Debye−Huckel scaling in protein folding kinetics is even more poorly explored but may also prove common. Two well-established examples involving NaCl have been reported to date: the rate of the slower of two folding phases of hen egg white lysozyme is reported to obey Debye−Huckel scaling (*22*), as is the rate of S-peptide association with the S-protein (*14*). Similarly, while square root dependence has not been explicitly reported for the folding of other proteins, inspection of the relevant published data suggests that the folding of cytochrome c_{551} (Figure 4 of ref *23*) and the unfolding of RNase T1 (Figure 5 of ref *19*, but see also ref *20*) also appear to exhibit at least approximately square root dependencies on ionic strength, suggesting that these systems, too, may obey the Debye−Huckel limiting law.

The discrepancy between the electrostatic β_{DH} and chaotropic β_T values, which presumably represent the "degree of consolidation" of electrostatic and hydrophobic interactions in the folding transition state, may also prove to be common. For example, Luisi and Raleigh have used the pH

Table 1

	chaotrope [kcal/(mol·M)]		ionic [kcal/(mol·M$^{1/2}$)]		chaotrope	ionic
	m_f	m_{eq}	m_f'	m_{eq}'	β_T	β_{DH}
urea	-0.52 ± 0.03	-0.62 ± 0.03			0.84	
NaCl			1.40 ± 0.06	2.90 ± 0.07		0.48
GuHCl	-2.1 ± 0.2	-2.9 ± 0.6	2.0 ± 0.4	4.0 ± 2.9	$\sim$0.72	$\sim$0.50

dependence of native state stability and folding rates to determine that the electrostatic interactions of glutamate and aspartate are only one-third as well formed in the folding transition state of the protein NTL9 as they are in the native state (*24*). This contrasts significantly with the 0.64 ratio reported for the extent of hydrophobic burial (as measured by the effects of urea). Similar pH- and chaotrope-derived inconsistencies occur in the folding of CI2 [0.28 versus 0.60 (*25*, *26*)] and barnase [0.47 versus 0.75 (*26*, *27*)]. Only for the protein CTL9 (*28*) do the pH- and chaotrope-derived β-values approach equality (at $\beta \sim 0.6$). Given that the formation of the hydrophobic interactions is thought to require close physical contact between residues, in contrast to the much longer range of electrostatic forces, the origins of this relatively general inconsistency may not be trivial. It presumably arises, however, due to the nonuniform distribution of charged and hydrophobic residues along the polypeptide chain, which allows favorable hydrophobic interactions to form without requiring the commensurate formation of unfavorable electrostatic interactions (*24*, *26*).

The effects of the chaotropic salt GuHCl on the (log) folding kinetics of the FynSH3 domain are reasonably well fitted as the sum of two effects, one of which is linear in concentration, presumably reflecting the chaotropic character of the salt, and one that exhibits a square root dependence expected for electrostatic screening. A similar linear plus square root dependency has been reported for the effects of GuHCl on the rate and thermodynamics of S-peptide association with the S-protein (*14*), and a dual linear model has been reported to fit the thermodynamics of helix formation (*29*). Above 1 M GuHCl the square root dependence begins to approximate linear dependence, and thus the sum of these two effects is also well approximated as linear. This accounts for the linear chevron behavior observed (*4*, *25*) for most small proteins in GuHCl. As shown here, however, a square root dependence can dominate the shape of the chevron at very low GuHCl concentrations, producing significant rollover. Because of this, GuHCl chevrons collected only over the linear region overestimate the folding rate of FynSH3 in the absence of denaturant by a factor of $\sim$5 and underestimate unfolding rates by a factor of $\sim$20 (compare Figure 5 versus Figure 6). GuHCl-induced overestimates or underestimates of folding and unfolding rates have previously been reported for other proteins (e.g., refs *23*, *30*, and *31*), as has similar rollover in GuHCl dependence of the folding free energy of ubiquitin (*32*) and acid-unfolded apomyoglobin and cytochrome *c* (*33*).

The low ionic strength buffer we have employed enhances the observed kinetic rollover, which even under these favorable conditions is apparent only at relatively low denaturant concentrations. This is highlighted by the work of Raleigh and co-workers (*24*, *28*), who report that in the presence of 100 mM NaCl the folding of both the N- and C-terminal domains of ribosomal protein L9 exhibits perfectly linear chevron behavior down to 0 M GuHCl. Nevertheless, it is quite possible that, for proteins exhibiting significantly greater electrostatic repulsion than FynSH3, this effect could be apparent even at higher ionic strengths. Our results thus suggest that, as is true with GuHCl melt-derived stability measurements (e.g., refs *19*, *20*, *38*, and *39*), caution is in order when extrapolating GuHCl-based chevrons to estimate folding rates in the absence of denaturant and in interpreting deviations from chevron linearity as evidence for non-two-state kinetics.

ACKNOWLEDGMENT

The authors thank Henry Orland, Jacob Israelachvili, and Angel Garcia for motivating this project and Ralph Reid for initial help with the characterization of the system. We also thank Jonathan Kohn for providing the NΔ3-FynSH3 mutant.

REFERENCES

1. Krantz, B. A., and Sosnick, T. R. (2001) Engineered metal binding sites map the heterogeneous folding landscape of a coiled coil, *Nat. Struct. Biol. 8*, 1042−1047.
2. Hofmeister, F. (1888) Zur Lehre von der wirkung der salze, II, *Arch. Exp. Pathol. Pharmakol. 24*, 247−260.
3. Timasheff, S. N. (1993) The control of protein stability and association by weak interactions with water: how do solvents affect these processes?, *Annu. Rev. Biophys. Biomol. 22*, 67−97.
4. Jackson, S. E. (1998) How do small single-domain proteins fold?, *Folding Des. 3*, R81−R91.
5. Silow, M., and Oliveberg, M. (1997) Transient aggregates in protein folding are easily mistaken for folding intermediates, *Proc. Natl. Acad. Sci. U.S.A. 94*, 6084−6086.
6. Dominy, B. N., Pearl, D., Schmid, F. X., and Brooks, C. (2002) The effects of ionic strength on protein stability: the cold shock protein family, *J. Mol. Biol. 321*, 541−554.
7. Debye, P., and Huckel, E. (1923) The interionic attraction theory of deviations from ideal behavior in solution, *Phys. Z. 24*, 185−206.
8. Plaxco, K. W., Guijarro, J. I., Morton, C. J., Pitkeathly, M., Campbell, I. D., and Dobson, C. M. (1998) The folding kinetics and thermodynamics of the Fyn-SH3 domain, *Biochemistry 37*, 2529−2537.
9. Pace, C. N. (1990) Conformational stability of globular proteins, *Trends Biochem. Sci. 15*, 14−17.
10. Gloss, L. S., and Placek, B. J. (2002) The effect of salt on the stability of the h2a−h2b histone dimer, *Biochemistry 41*, 14951−14959.
11. Pradeep, L., and Udgaonkar, J. B. (2002) Differential salt-induced stabilization of structure in the initial folding intermediate ensemble of barstar, *J. Mol. Biol. 324*, 331−347.
12. Myers, J. K., Pace, C. N., and Scholtz, J. M. (1995) Denaturant *m* values and heat capacity changes: Relation to changes in accessible surface areas of protein unfolding, *Protein Sci. 4*, 2138−2148.
13. Olivberg, M., Vuilleumier, S., and Fersht, A. R. (1994) Thermodynamic study of the acid denaturation of barnase and its dependence on the ionic strength: evidence for residual electrostatic interactions in the acid/thermally denatured state, *Biochemistry 33*, 8826−8832.
14. Goldberg, J. M., and Baldwin, R. L. (1998) Kinetic mechanism of a partial folding reaction. 1. Properties of the reaction and effects of denaturants, *Biochemistry 37*, 2546−2555.
15. Perl, D., and Schmid, F. X. (2001) Electrostatic stabilization of a thermophilic cold shock protein, *J. Mol. Biol. 313*, 343−357.

16. Nishimura, C., Uversky, V. N., and Fink, A. L. (2001) Effect of salts on the stability and folding of staphylococcal nuclease, *Biochemistry 40*, 2113−2128.
17. Chen, Y., and Clark, A. C. (2003) Equilibrium and kinetic folding of a α-helical greek key protein domain: Caspase recruitment domain (CARD) of RICK, *Biochemistry 42*, 6310−6320.
18. Johnson, C. M., Cooper, A., and Stockley, P. G. (1992) Differential scanning calorimetry of thermal unfolding of the methionine repressor protein (MetJ) from *Escherichia coli*, *Biochemistry 31*, 9717−9724.
19. Mayr, L. M., and Schmid, F. X. (1993) Stabilization of a protein by guanidinium chloride, *Biochemistry 32*, 7994−7998.
20. Yao, M. Y., and Bolen, D. W. (1995) How valid are the denaturant-induced unfolding free energy measurements? Level of conformance assumptions over an extended range of ribonuclease A stability, *Biochemistry 34*, 3771−3781.
21. Maldonado, S., Irun, P. M., Campos, A. L., Rubio, A. J., Luquita, A., Lostao, A., Wang, R., Garcia-Moreno, B. E., and Sancho, J. (2002) Salt-induced stabilization of the apoflavodoxin at neutral pH is mediated through cation-specific effects, *Protein Sci. 11*, 1260−1273.
22. Itzhaki, L. S., Evans, P. A., Dobson, C. M., and Radford, S. E. (1994) Tertiary interactions in the folded pathway of hen lysozyme: kinetic studies using fluorescent probes, *Biochemistry 33*, 5212−5220.
23. Gianni, S., Brunori, M., and Travaglini-Allocatelli, C. (2001) Refolding kinetics of cytochrome c_{551} reveals a mechanistic difference between urea and guanidine, *Protein Sci. 10*, 1685−1688.
24. Luisi, D. L., and Raleigh, D. P. (2000) pH-Dependent interactions and the stability and folding kinetics of the N-terminal domain of L9. Electrostatic interactions are only weakly formed in the transition state for folding, *J. Mol. Biol. 299*, 1091−1100.
25. Jackson, S. E., and Fersht, A. R. (1991) Folding of chymotrypsin inhibitor 2. 1. Evidence for a two-state transition, *Biochemistry 30*, 10428−10435.
26. Olivberg, M., and Fersht, A. R. (1996) Formation of electrostatic interactions on the protein-folding pathway, *Biochemistry 35*, 2726−2737.
27. Tan, Y. J., Oliveberg, M., and Fersht, A. R. (1996) Titration properties and thermodynamics of the transition state for folding: comparison of two-state and multi-state folding pathways, *J. Mol. Biol. 264*, 377−389.
28. Sato, S., and Raleigh, D. P. (2002) pH-dependent stability and folding kinetics of a protein with an unusual alpha-beta topology: the C-terminal domain of the ribosomal protein L9, *J. Mol. Biol. 318*, 571−582.
29. Smith, J. S., and Scholtz, J. M. (1996) Guanidine hydrochloride unfolding of peptide helices: separation od denaturant and salt effects, *Biochemistry 35*, 7292−7297.
30. Otzen, D. E., and Oliveberg, M. (2001) A simple way to measure protein refolding rates in water, *J. Mol. Biol. 313*, 479−483.
31. Sridevi, K., and Udgaonkar, J. B. (2002) Unfolding rates of barstar determined in native and low denaturant conditions indicate the presence of intermediates, *Biochemistry 41*, 1568−1578.
32. Ibarra-Molero, B., Loladze, V. V., Makhatadze, G. I., and Sanchez-Ruiz, J. M. (1999) Thermal versus guanidine-induced unfolding of ubiquitin. An analysis in terms of the contributions from charge−charge interactions to protein stability, *Biochemistry 38*, 8138−8149.
33. Hagihara, Y., Aimoto, S., Fink, A. L., and Goto, Y. (1993) Guanidine hydrochloride-induced folding of proteins, *J. Mol. Biol. 231*, 180−184.
34. Khorasanizadeh, S., Peters, I. D., Butt, T. R., and Roder, H. (1993) Folding and stability of a tryptophan-containing mutant of ubiquitin, *Biochemistry 27*, 7054−7063.
35. Krantz, B. A., Mayne, L., Rumbley, J., Englander, S. W., and Sosnick, T. R. (2002) Fast and slow intermediate accumulation and the initial barrier mechanism in protein folding, *J. Mol. Biol. 324*, 359−371.
36. Shastry, M. C. R., and Udgaonkar, J. B. (1995) The folding mechanisms of barstar−evidence for multiple pathways and multiple intermediates, *J. Mol. Biol. 247*, 1013−1027.
37. Carrion-Vazquez, M., Oberhauser, A. F., Fowler, S. B., Marszalek, P. E., Broedel, S. E., Clarke, J., and Fernandez, J. M. (1999) Mechanical and chemical unfolding of a single protein: A comparison, *Proc. Natl. Acd. Sci. U.S.A. 96*, 3694−3699.
38. Monera, O. D., Kay, C. M., and Hodges, R. S. (1994) Protein denaturation with guanidine hydrochloride or urea provides a different estimate of stability depending on the contributions of electrostatic interactions, *Protein Sci. 3*, 1984−1991.
39. DeKoster, G. T., and Robertson, A. D. (1997) Calorimetrically-derived parameters for protein interactions with urea and guanidine-HCl are not consistent with denaturant *m* values, *Biophys. Chem. 64*, 59−68.
40. Atkins, P. (1998) *Physical Chemistry*, 6th ed., pp 249−253, W. H. Freeman and Co., New York.

BI048444L